The paper was published in the proceedings of the 7th International Conference on Earthquake Geotechnical Engineering and was edited by Francesco Silvestri, Nicola Moraci and Susanna Antonielli. The conference was held in Rome, Italy, 17 – 20 June 2019.

Earthquake Geotechnical Engineering for Protection and Development of Environment and Constructions – Silvestri & Moraci (Eds)
© 2019 Associazione Geotecnica Italiana, Rome, Italy, ISBN 978-0-367-14328-2

An innovative solution for the retrofitting of an existing railway embankment

V. Cefaliello
Rete Ferroviaria Italiana S.p.A, Regional Direction, Bologna, Italy

R. Di Francesco
Paolo Petrella Engineering, Italy
E. Lolli & G. Nestovito
Rete Ferroviaria Italiana S.p.A, Regional Direction, Bologna, Italy

P. Petrella
Paolo Petrella Engineering, Italy

ABSTRACT: As part of the exceptional maintenance of the Italian railway line Bologna-Milan, it was necessary to solve a seismic geotechnical problem attributable to the extreme complexity of the alluvial subsoil. Indeed, from the processing data recorded during on-site and laboratory tests, the subsoil results characterized by both extreme stratigraphic and physical-mechanical variations. An innovative consolidation solution of the embankment was adopted, which involves in the construction of a double bulkheads, realized with steel micro-piles, mutually constrained with horizontal tie rods. The complexity of performed structure can be summarized in: i) execution of the construction work in presence of rail traffic, which strongly forced the technical solution adopted; ii) installing of fiberglass tubes infill and pressure injection of consolidating mixture inside the embankment to increase the soil stiffness; iii) adoption of glass fiber composites for the construction of tie rods, to remove the problem of transmission stray electrical currents. The last point was solved through micromechanical design of a composite fiberglass material. The work was completed within the scheduled timeframe eliminating the interference with the railway operation.

1 INTRODUCTION

During the maintenance of the Italian high-speed/high-capacity Bologna-Milan railway line, it was necessary to retrofit an existing railway embankment with failures of both platform and escarpments, attributable to the high compressibility of alluvial foundation soils. Since it was impossible to refer to a rigid base layer confined to a shallow depth, the influence of kinematic constraints on soils mechanical behavior has been considered as technical solution (Figure 1). The soil activity is not unequivocal but varies from a condition with two degrees of freedom (cylindrical compression conforming to the Poisson solid, with degeneration of stiffness) to a condition with only one degree of freedom (or uniaxial deformation, with material hardening).

The present work illustrates the synthesis of a geotechnical study whose complexity can be summarized in 6 steps (Figure 2): 1) the site is located 36 km from the earthquake epicenter of 20 May 2012 with M_w 5.8 and 27 km from the following earthquake of 29 May with Mw 5.6; 2) the construction works were carried out without interruptions of railway traffic that, together with the mentioned geological conditions, strongly constrained the technical solution; 3) the designed solution consisted in a pair of mutually winched bulkheads with horizontal fiberglass tie rods, in order to allow the development of a single degree of freedom; 4) the bulkheads were made with steel micropiles arranged in quincunx position, being able to use only small drilling machines capable of satisfying the first step; 5) the construction of anchoring beams (and related vertical wall excavations) required a prior consolidation of the embankment by injections of consolidating mixture whose choice, compared to other materials, depended on the porosity and

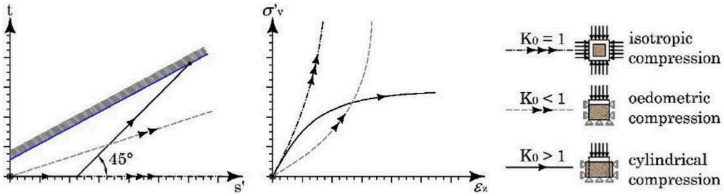

Figure 1. The comparison between the isotropic, edometric and cylindrical stress paths reveals different mechanical behaviors which depend on the applied constraint (Di Francesco, 2014).

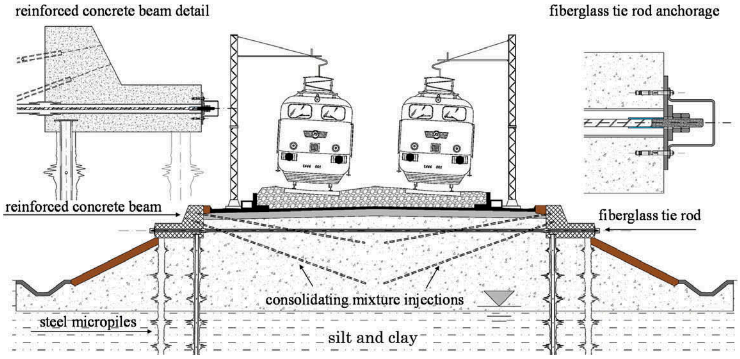

Figure 2. Typology section of the geotechnical structure with detail of reinforced concrete beams, injections of consolidating mixture and anchoring system with composite tie rods.

permeability of geomaterials; 6) the presence of stray currents, due to the power supply for trains, prevented the use of steel tie rods and required the design of a fiberglass rod that would meet the particular design and maintenance requirements.

Despite the use of complex finite element models based on Continuum Mechanics are capable of simulating the effects over time of cement injections and differential displacements between rails and soil during the various executive phases, the design of the tie rods was carried out using the Fracture Mechanics. In this manner, it was possible to obtain a high reliability of the geotechnical structures and a necessary simplification of the control and maintenance of the single reliable structural elements also to technicians who are not necessarily expert.

2 CONSTRUCTION OF GEOTECHNICAL MODEL

2.1 *Brief geological notes*

The Bologna-Milan railway line was built along a transition zone between the Apennine mountain and the front of a flood plain. From a sedimentological point of view, the transition belt is occupied by a series of coalescing conoids characterized by deposition of mainly coarse soils near the top. Those soils, become increasingly fine with the approach to alluvial deposits of a flood plain, with which they are interdigitated. In the case of the embankment studied, the geological investigations have highlighted its location at the base of one conoids, whose subsoil is characterized by the presence of compressive clay limes with a thickness of 32 meters (followed by sand and gravel). Moreover, inside sandy lenses have been recorded. The piezometric level is close to the topographic surface, with seasonal oscillations of about one meter.

2.2 *Geotechnical modeling*

The geotechnical model was constructed re-analyzing the numerous investigation available for the design of embankment, consisting logging drillings, laboratory tests (edometric and triaxial tests) and on-site CPTu tests.

The faced problems mainly concerned the calibration of the physical-mechanical parameters, given an evident subsidence in progress, and the construction of finite element models supporting geotechnical and structural design. Therefore, in order to capture the salient aspects of the problem by numerical model, an iterative procedure was used. Indeed, studying the behavior of existing geotechnical structures and the soils interaction, the FEM model evolves through calibration steps among numerical solutions, monitoring, in situ and laboratory tests (Dolezalova et al., 2001). In short, physical-mechanical behavior of the embankment and foundation soil was codified with a preliminary FEM model (which simulated the construction of the embankment and its operation), assembled starting from experimental data (geognostic surveys) and calibrated through the measurement of subsidence. Moreover, the model was improved with a topographical investigation by GPS ground conjugated with aerial shots performed with drones. To achieve the goal, which was able to provide physico-mechanical data useful to design the consolidation intervention through FEM models, it was necessary to explore various constitutive laws available in literature. In order to grasp both the initial degenerative behavior of the foundation soil (subjected to a compression pressure path) and the hardening one associated with the lateral confinement imposed by the geotechnical structure has been adopted: a) the perfectly plastic nonlinear elastic bond of Mohr-Coulomb (1900) to simulate the embankment behavior; b) the plastic-hardening linkage/softening Cap-Model to simulate the foundation soil, being based on an uncoated plastic flow law (Chen & Baladi, 1985 – Figure 3); c) the non-linear elastic bond for structural works; d) Biot's poroelastic theory (1956) to simulate both the permeation due to injections of consolidating mixture and the consolidation associated to the work.

Referring to Chen & Baladi (1985) for further details, the starting point is given by the determination of prestressing pressure by means of edometric tests, which allows to identify the intersection of elliptical cap with the p′ axis (Figure 3). With the triaxial tests are instead determined Equations 1 and 2:

$$\alpha = \frac{2sin\phi'}{(3+sin\phi')\sqrt{3}} \tag{1}$$

$$k = \frac{6c'\cos\phi'}{(3+sin\phi')\sqrt{3}} \tag{2}$$

where α identifies the slope of Drucker-Prager surface, which in the last conditions is reduced to α_u, that is reduced to the slope of Critical State Line.

The additional parameters to be determined are (Equations 3):

$$p_{cs} = p_c K_0;\;\; R_1 = p_c - p_{cs};\;\; R_2 = \sqrt{J_2};\;\; R = \frac{R_1}{R_2} \tag{3}$$

The results are summarized in Table 1.

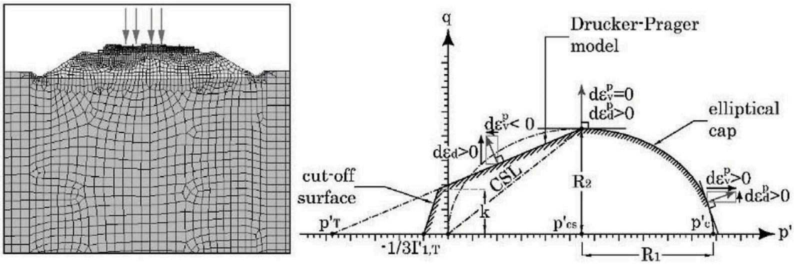

Figure 3. Left: detail of the FEM model to calibrate the physical-mechanical parameters; right: Cap-Model structure in the q-p′ plane used to model foundation soils (Chen & Baladi, 1985 - modified).

Table 1. Physico-mechanical parameters of foundation soils interpreted according to the Cap-Model.

γ [kN/m³]	c' [kPa]	ϕ' [°]	ν	E' [MPa]	c_c	p_c [kPa]	p_{cs} [kPa]	R_1 [kPa]	R_2 [kPa]	R [kPa]
19	2	24	0.37	4	0.324	90	53.37	36.63	21.14	1.73

3 COMPOSITE FIBERGLASS TIE RODS DESIGN

3.1 *Fundamental concepts: mixture law and micromechanical analysis*

In order to have electrically neutral tie rods, they were designed in fiberglass by applying two fundamental concepts: a) the mixtures law; b) the energetic balance at the base of Fracture Mechanics theory. For a length of 17.4 m and a design tensile load of 50 kN, a diameter of 30 mm was assumed (corresponding to a tensile stress σ_a = 70.8 MPa).

As regards the application of mixture law, it was assumed that the behavior of fiber composite tie was transversely isotropic, with elastic-mechanical characteristics depending on the matrix (polymer hardener resin) and the reinforcement (glass). Further, it was supposed that each mechanical parameter of the composite is a function of the volume for individual components, limiting the micromechanical analysis to the post-prototyping verification only. The starting features are summarized in Tables 2 and 3 according to the longitudinal direction only (E/γ = specific module, σ_r/γ= specific resistance).

In order to contain costs, a composite consisting of 60% polyester and 40% glass E (Table 2) has been designed, whose theoretical characteristics are summarized in Table 4. The design data were subsequently confirmed by stress tests.

On the other hand, the micromechanical analysis with an energetic approach originates from the studies of Griffith (1920) and Irwin (1958), on which the modern Fracture Mechanics was born; the starting point is the calculation of elastic deformation energy per unit of volume accumulated by a generic material subjected to a tensile stress:

$$U^* = \frac{1}{V}\int f dx = \int \frac{f}{A}\frac{dx}{L} = \int \sigma\, d\varepsilon \tag{4}$$

for a material that follows the linear elastic law of Hooke, Equation 4 becomes:

$$U^* = \frac{\sigma^2}{2E} \tag{5}$$

In order to understand what happens with the presence of an amplitude crack, it is useful to refer to Roylance (2001). Indeed, it emerges the presence of two roughly triangular areas,

Table 2. Mechanical characteristics of glass compared to steel material.

Material	γ [kN/m³]	E [MPa]	σ_r [MPa]	E/γ [m]	σ_r/γ [m]
Glass E	25,4	72400	3500	2850,4	137,8
Glass S	24,8	85500	4600	3447,6	185,5
Steel	78	210000	590	2692,3	7,6

Table 3. Mechanical characteristics of matrix.

Material	γ [kN/m³]	E [MPa]	σ_r [MPa]	E/γ [m]	σ_r/γ [m]
Epoxy	12	4500	130	375	10,8
Vinylester	12	4000	80	333,3	6,7
Polyester	11,5	3300	75	287	6,5

Table 4. Mechanical characteristics of the composite material.

Material	γ [kN/m^3]	E [MPa]	σ_r [MPa]	E/γ [m]	σ_r/γ [m]
Composite	17.1	30940	1445	1809.4	84.5

whose sides are a e βa, completely discharged because they are subject to the release of energy elastic deformation. Considering the geometry issue, the solution conforms to the results of Inglis (1913), when $\beta = \pi$. Consequently, the deformation energy per unit of volume released during crack propagation is equal to Equation 6:

$$U^* = -\frac{\sigma^2}{2E}\pi a^2 \tag{6}$$

The creation and consequent growth of a crack, produces two new orthogonal surfaces to the traction plane, to which is associated the surface energy S (per unit of thickness). Once the surface energy γ (Joules/m^2) of the material it is known S becomes:

$$S = 2\gamma a \tag{7}$$

Ultimately, the total energy associated with a crack is given by the (positive) surface energy, absorbed to create the new surfaces, net of the (negative) deformation energy released in the neighboring regions:

$$U = S - U^* = 2\gamma a - \frac{\sigma^2}{2E}\pi a^2 \tag{8}$$

Equation 8 states that the crack is stable up to a certain length, beyond which it becomes unstable and therefore free to grow until the sheet collapses. As a consequence, in order to calculate the critical gap length:

$$\frac{\partial(S - U^*)}{\partial a} = 2\gamma - \frac{\sigma^2}{E}\pi a = 0 \tag{9}$$

Resolving Equation 8 as a function of the effort, σ is equal to:

$$\sigma = \sqrt{\frac{2E\gamma}{\pi a}} \tag{10}$$

The strategic importance of Equation (10) is inherent to determine a traction effort for which the cracks in the composite will always be stable, even during a usual inspections. Therefore, placed a = 0.001 m (1 mm) and γ =0.00079 J/m^2 (determined experimentally according to the ASTM D 3039/D 3039M standard), a critical effort of 124.8 MPa is obtained (higher than the design σ_a=70.8 MPa) being E deducible from Table 4 (in addition to tests performed on the prototypes). The result obtained implies that it is not necessary to calculate the safety coefficient with respect to the fracture, since for the applied stress the composite will be always stable.

4 RESULTS OF FEM MODELS

For the geotechnical and structural design, 2D and 3D FEM models have been realized. In particular, two parallel paths were followed which also had to take into account both the technical code in force in Italy and site seismicity: a) in the first, 2D FEM models were constructed to analyze post-intervention behavior as a function of the static and seismic ultimate limits. b) in the second, the 3D models have to simulate several construction phases and their influence on the inevitable displacements of the railway armament. In fact, it was necessary to take into account that consolidation developed during trains operation.

In the case of ultimate limit state analyzes (N.T.C, 2008), a routine calculation called c′-ϕ′ reduction was used. Progressively, it reduces the effective cohesion and the cutting resistance angle until the fracture is reached. The comparison for each calculation steps between the current stress diverter and the initial one has been defined (calculated for each node of mesh to provide a safety factor). For the analysis during transient, existence functions and load functions were used, associated with the different parts of the mesh. In this manner simulation of the construction phases and the design stresses have been performed. The analysis results (Figure 4) provided a safety factor F_s = 3.20 and armament displacements of a few millimeters, falling within the operating tolerances (i.e. corresponding to deviations that maintain established levels of circulation quality) and safety. Moreover, the results showed how the pretensioning of geotechnical structure by means of composite tie-rods, keeps the soil in a state of perennial compression and in a 1D deformation condition according to Figure 1.

Regarding the analysis of ground-structure interaction in seismic perspective, it was necessary to take into account the Emilia's earthquakes recorded in 2012, since the expected regulatory accelerations for the site (between 0.118 and 0.157g) are turned out to be lower than those actually measured (Figure 5a).

A further problem, is derived from the high thickness of alluvial soils, with the rocky substratum, constituting the place of propagation of the earthquake, located hundreds of meters deep. This, prevented the construction of a mesh whose base corresponded to the flood-substrate passage (constituting the entry point of the design earthquake), as it would have required the use of tens of thousands of nodes with an excessive computational burden. To overcome these limitations, a mesh of a thickness with 32 meters was built, provided with hinges on the base and viscous dampers on the side edges, in order to simulate the energy dispersion by irradiation (Nuti & Pinto, 1990). Considering the presence of rigid constraints at the base of the mesh (whose effects in terms of reflections of the seismic waves are however mitigated by the high internal damping of the ground due to their high deformability), the accelerograms of Figure 5a have been applied and progressively scaled up to the real accelerations measured on the ground.

Both dynamic analysis (performed by integration with the design accelerogram steps) and simulation of the viscous dampers on mesh edges, required the Rayleigh damping matrix (1877) present in the general equation of motion:

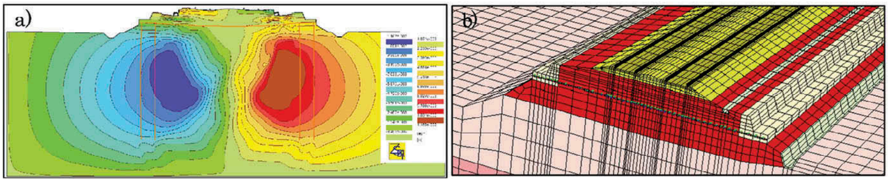

Figure 4. a) compression state induced by the pretensioning of composite tie rods; b) 3D model for the analysis during construction phases.

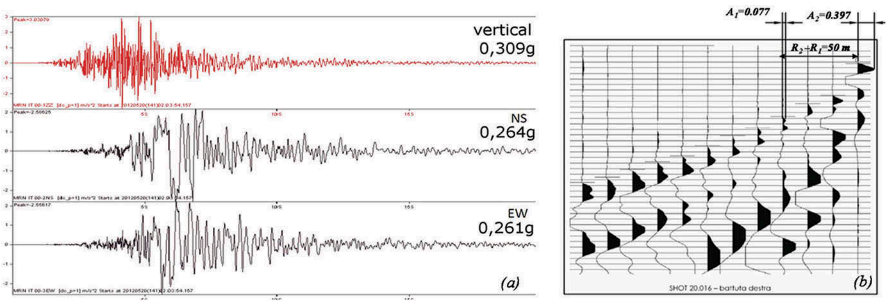

Figure 5. *a)* Emilia's earthquake accelerograms of 20th May 2012 with M_w=5.8 (Martelli, 2013); *b)* seismogram derived from the execution of a seismic refraction.

$$[C] = \alpha[M] + \beta[K] \tag{11}$$

where α and β are two constants which depend on the soils internal damping and their modes of vibration, described by the angular pulsation:

$$\alpha + \beta\omega_i^2 = 2\omega_i\xi \tag{12}$$

from Equation 12 the internal damping is obtained:

$$\xi = \alpha/2\omega_i + \beta\omega_i/2 \tag{13}$$

For the determination of internal damping, the seismic signal attenuation coefficient method was used increasing distance *R* from the source (Bornitz, 1931):

$$\xi = \ln(A_1R_1/A_2R_2)/R_2 - R_1 \tag{14}$$

$$\alpha = \xi(2\omega_1\omega_2/\omega_1 + \omega_2) = 0.298;\ \beta = \xi(2/\omega_1 + \omega_2) = 0.013 \tag{15}$$

where A_1 and A_2 represent the amplitude of two seismic signals placed at distance R_1 and R_2 from the source (Figure 5b). The problem was resolved performing vibrometric measurements on the ground to determine the fundamental frequencies (f_1 = 0.44 Hz, ω_1 = 2.76 rad/sec; f_2 = 1.31 Hz, ω_2 = 8.23 rad/sec). In addition to the refractive seismic survey in Figure 5b and inserting the combination of data in the Equation (14) were obtained: ξ =7.2 %.

With the determination of ξ it was possible to carry out the dynamic analysis of the problem. The results shown that the two bulkheads represented in Figure 2, always oscillate in phase, keeping the grounds inside them in a constant state of compression. However, for brevity, the complete results achieved, in a subsequent work will be treated.

5 THE CONSTRUCTION PHASES

The consolidation design of the embankment has been carefully studied to allow the construction during normal railway operation respecting all the strict safety procedures defined by the infrastructure network manager (Standard of Rete Ferroviaria Italiana, 2017). The Italian Railway company, supported the innovative design to increase structural performance of the embankment without ever affecting both safety building site and trains operation. In particular, the train safety was guaranteed by installing a monitoring system before working to measure rails displacements at any time. During the 3 months prior to the consolidation work, the movements of the train track were recorded and a safety thresholds were defined. In this way it was possible to check the altimetry progress level during the construction operations. The processing construction steps are briefly summarized in the following order (Figure 6): (i) realization of the building site and installation of steel micro-piles; (ii) construction of the reinforcement stands and realization of holes, with drilling machines, into the embankment; (iii) installation of fiberglass rods protected by PEAD pipes; (iv) tightening of the tie rods and dismantling of the building site.It is important to highlight that only during phase (ii) the work was carried out during the ordinary maintenance of the railway line that is without the traffic trains. Moreover, in this phase, a tamping machine for recovering possible track faults has been provided. The work was carried out in about six months. Simultaneous use of two drilling machines to make the 250

Figure 6. Advancement work for the embankment consolidation with the innovative system.

steel micro-piles with a depth of 10 meters were used. The casting of about 500 m^3 of concrete C28/35 with 135000 kg of B450C steel bars have been used. Nowadays, after approximately 4 months from works end, the installed monitoring has highlighted the settling of the railway embankment, eliminating the registered displacements before the intervention.

6 CONCLUSIONS

Strategic infrastructure management requires innovative and sustainable technological solutions (Nestovito, 2016 and Mezzi, 2018). Dealing with maintenance scenarios and new seismic conditions, the new system implemented, guarantees the safety of the railway train operation during the consolidation without creating line interruptions. Moreover, with the new materials used, fiberglass rods, the problems of stray currents that prevent the use of steel ones have been eliminated. The system implemented is being employed on other railway tracks with different types of soils with similar issues. Finally, in order to be able to use the new system in other recurrent problems on railway embankments, further studies are necessary.

ACKNOWLEDGEMENT

This research has been funded by the Italian Railway Company (Rete Ferroviaria Italiana S.p. A.) and we are grateful to the Ceprini Costruzioni S.r.l. company for the realization of embankment consolidation and Top Glass S.p.A. Industries to the production of fiberglass rods.

REFERENCES

Biot, M.A. 1956. *Theory of deformation of a porous viscoelastic anisotropic solid*. Journal of Applied Physics, 27(5), pp. 459–467.

Bornitz, G. 1931. *Uber die Ausbreitung dor vor Groszkolbenmaschinen erseugten Bodenschwingungen in die Tiefe*. Berlin: Springen.

Chen, W.F. & Baladi, G.Y. 1985. *Soil Plasticity: Theory and Implementation*. Amsterdam: Elsevier Science Publisher.

Di Francesco, R.; Siena, M.; Tiberii, M.G.; Labagnara, R.; Di Matteo, L.; Scalella, G.; 2001. Il contributo della geotecnica nella comprensione dei dissesti storici dell'abitato di Campli. In, *Sicurezza ed adeguamento delle opera esistenti; XXII Convegno Nazionale di Geotecnica*. Bologna: Patron Editore.

Dolezalova, M.; Hladik, I.; Zemanova, V.; Danko, J.; 2001. Problem solving by interactive use of numerical models and field measurement. In, *Proceedings X International Conference of computer methods and advances geomechanics, Tucson, Vol. 1, 39–48*. Rotterdam: Balkema.

Griffith, A.A. 1920. *The fhenomena of rupture and flow in solids*. Transaction, Royal Society of London.

Inglis, C.E. 1913. *Stresses in a plate due to the presence of cracks and sharp corners*. Proc. Inst. Naval Architects, vol. 60, pp 219–241.

Irwin, G.R. 1958. *Fracture. Encyclopedia of Physical*. Berlin: Springer-Verlag.

Martelli, L. 2013. Course of seismic microzonation and evaluation of the local seismic response for post-earthquake reconstruction: the earthquake of Emilia. University of L'Aquila.

Mohr, O. 2001. *Welche Umstände bedingen die Elastizitägrenzee und den Bruch eines Materials*. Zeitschr Vereines deutsch. Ingenieure, 44, 1–12.

Mezzi, M.; Nestovito, G.; Petrella, P.; Cefaliello, V. 2018. Innovative Suspended Superstructure for the Retrofitting of a Steel Truss Railway Bridge,*Key Engineering Materials*,Vol.763, pp.1121–1128, 2018

National Technical Code for construction (NTC). The Italian Ministry of Infrastructure, 2008.

Nestovito, G. & Occhiuzzi, A. 2016. Implementation of smart-passive dampers combined with double concave friction pendulum devices to retrofit an existing highway viaduct exploiting the seismic early warning information. In *Engineering Structures*, Elsevier, Volume 120, pages: 58–74.

Nuti, C.; Pinto, P.E.; 1990. Analisi dell'interazione terreno-struttura in condizioni sismiche. In, Interazione terreno-struttura in prospettiva sismica. Udine: International Center for Mechanical Sciences.

Rayleigh, L. 1877. *Theory of Sound*. Dover Publication, New York, 145, re-issue.

Roylance, D. 2001. *Introduction to Fracture Mechanics*. Department of Materials Science and Engineering, Massachusetts Institute of Technology, MA 02139.

Standard of RFI DTC INC CS IFS 001 A, "Design and construction of railway structures", RFI S.p.A..